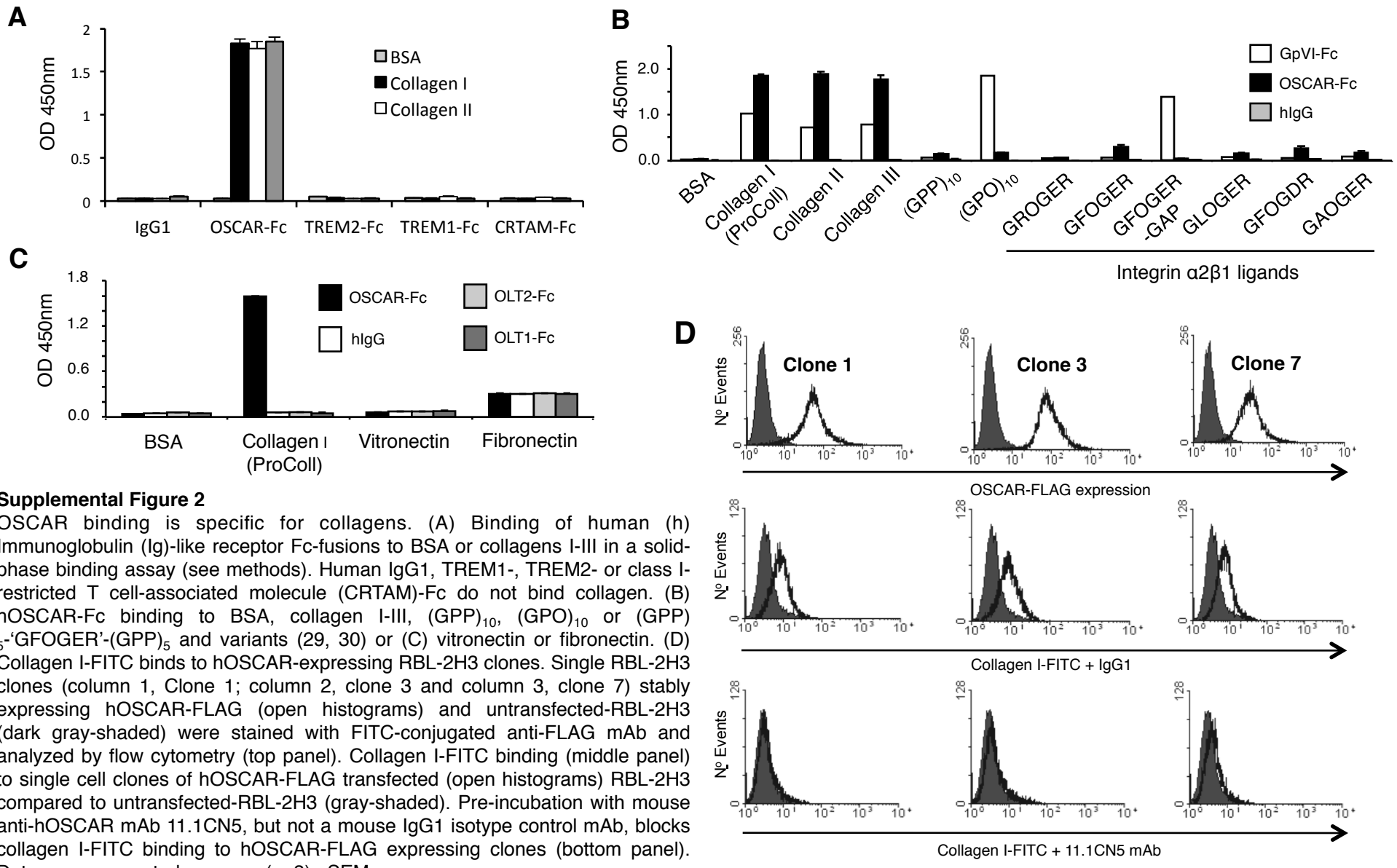


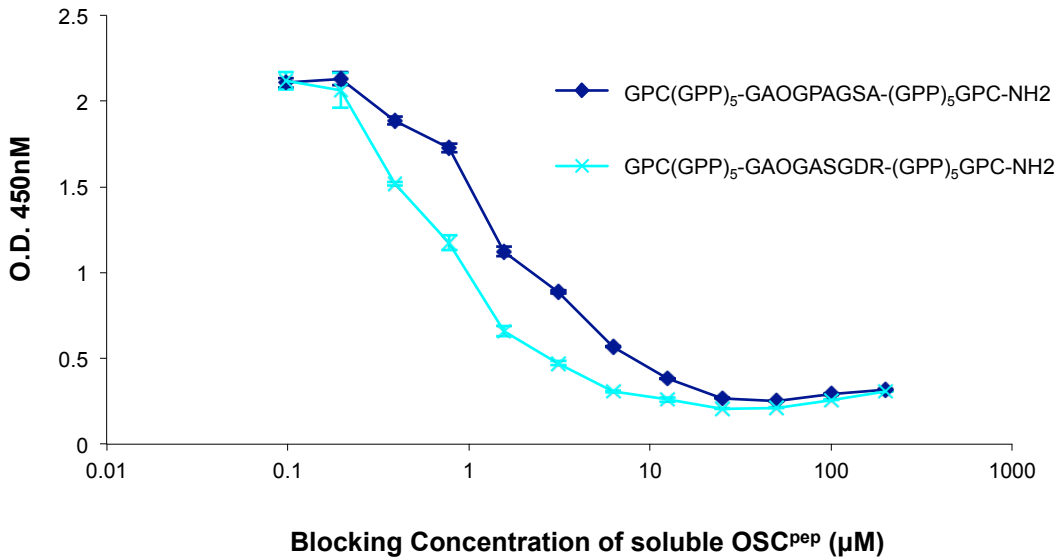
### Supplemental Figure 1

ITAM receptors co-stimulate RANK for osteoclastogenesis. Osteoclast precursors can be delivered to bone surfaces either via capillaries or from the bone marrow. Native bone (light blue) surfaces are coated with a layer of fibrillar collagen (brown), which is covered by a layer of osteoblastic bone-lining cells and stromal cells. Microendothelial cells, stromal cells and osteoblast-lineage cells (e.g. bone-lining cells) can express the cytokine, Receptor Activator of NF-KB-ligand (RANKL, black squares), and are associated with ligands for co-stimulatory receptors, such as the Osteoclast-associated receptor (OSCAR) or the triggering receptor expressed on myeloid cells (TREM)-2. OSCAR and TREM-2 specifically associate with adaptors encoding Immunoreceptor Tyrosine-based Activation Motif (ITAM, open squares), such as the Fc receptor common γ chain (FcRy) and the DNAX-activating protein of 12kDa (DAP12). RANKL binding to RANK on pre-osteoclasts results in a signal cascade, which converges on the transcription factor, NFATc1. Ligands for co-stimulatory receptors induce intracellular ITAM signaling, characterized by activation of phospholipase C (PLC)-γ by Tec kinases and release of calcium from intracellular stores. Calcium-dependent activation of NFATc1 results in auto-amplification and further up-regulation of osteoclast-specific genes, with subsequent progression to terminal osteoclast differentiation, characterized by pre-osteoclast cell fusion and multinucleation on bone surfaces.



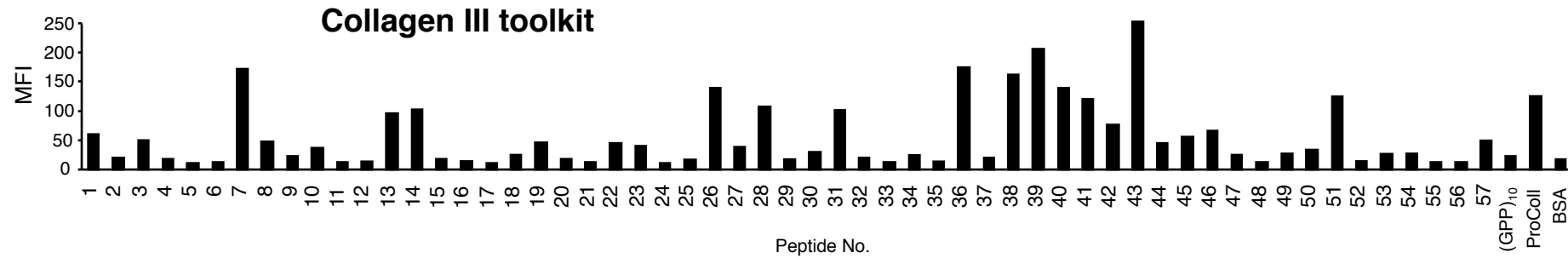
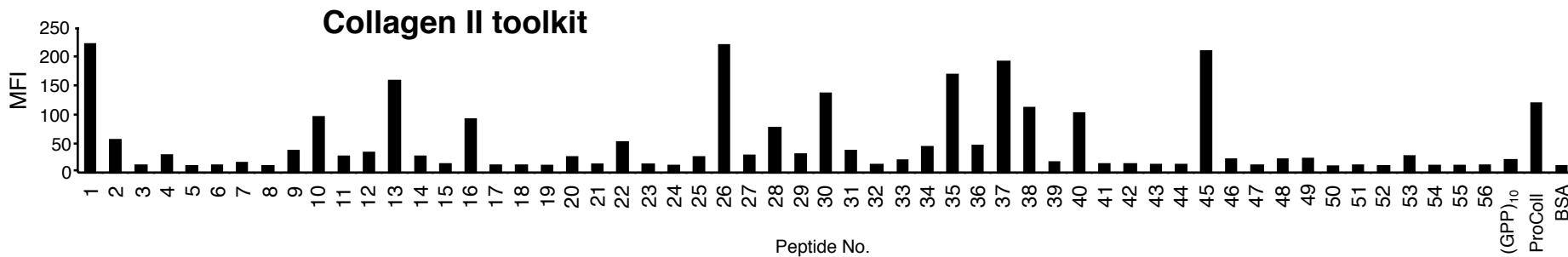
**Supplemental Figure 2**

OSCAR binding is specific for collagens. (A) Binding of human (h) Immunoglobulin (Ig)-like receptor Fc-fusions to BSA or collagens I-III in a solid-phase binding assay (see methods). Human IgG1, TREM1-, TREM2- or class I-restricted T cell-associated molecule (CRTAM)-Fc do not bind collagen. (B) hOSCAR-Fc binding to BSA, collagen I-III,  $(GPP)_10$ ,  $(GPO)_10$  or  $(GPP)_5$ -‘GFOGER’-(GPP)<sub>5</sub> and variants (29, 30) or (C) vitronectin or fibronectin. (D) Collagen I-FITC binds to hOSCAR-expressing RBL-2H3 clones. Single RBL-2H3 clones (column 1, Clone 1; column 2, clone 3 and column 3, clone 7) stably expressing hOSCAR-FLAG (open histograms) and untransfected-RBL-2H3 (dark gray-shaded) were stained with FITC-conjugated anti-FLAG mAb and analyzed by flow cytometry (top panel). Collagen I-FITC binding (middle panel) to single cell clones of hOSCAR-FLAG transfected (open histograms) RBL-2H3 compared to untransfected-RBL-2H3 (gray-shaded). Pre-incubation with mouse anti-hOSCAR mAb 11.1CN5, but not a mouse IgG1 isotype control mAb, blocks collagen I-FITC binding to hOSCAR-FLAG expressing clones (bottom panel). Data are represented as mean (n=3)  $\pm$  SEM.



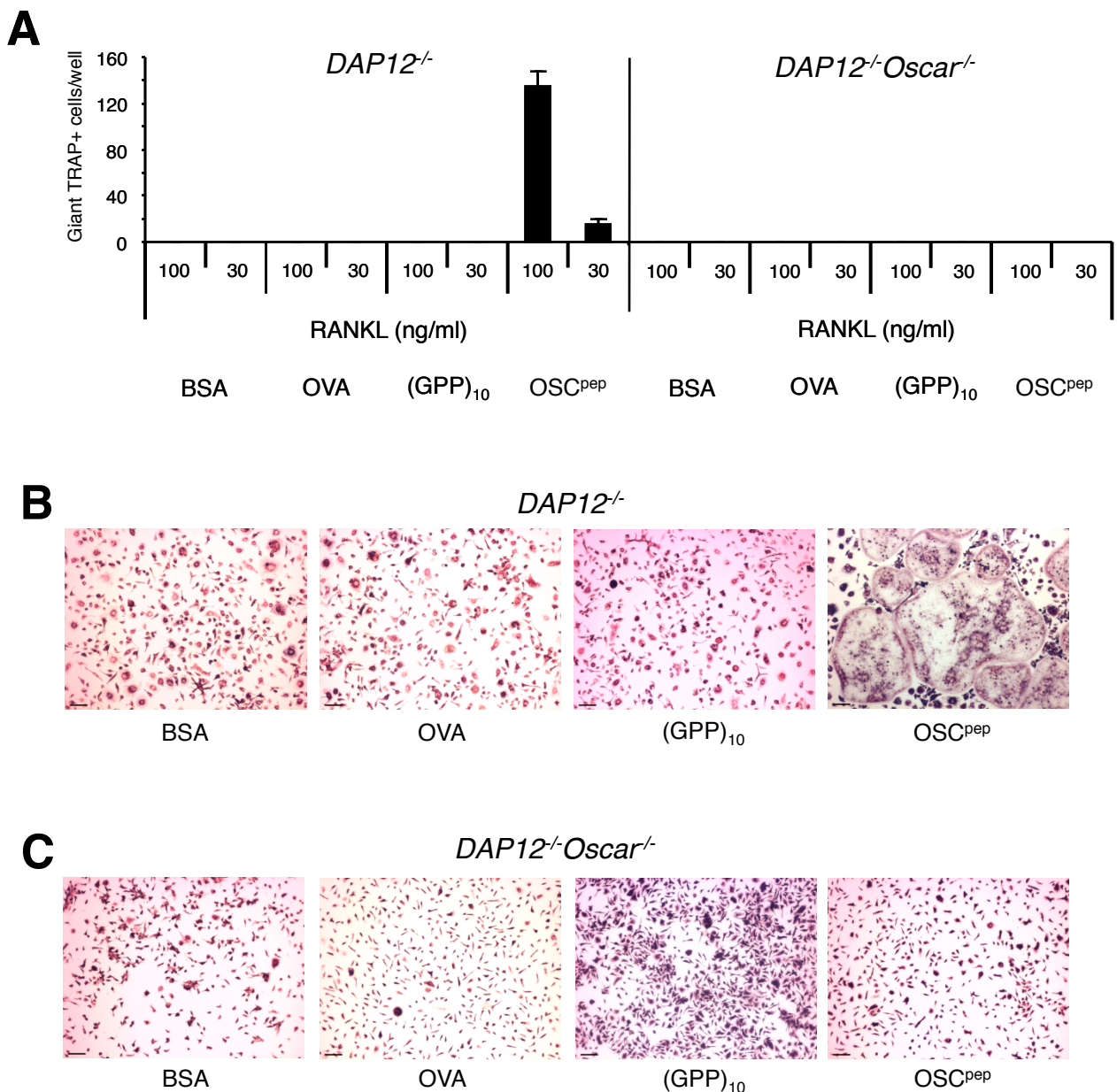
### Supplemental Figure 3.

OSCAR binding to its cognate triple-helical collagen motif is dissociable. Soluble OSC<sup>pep</sup> can block OSCAR-Fc binding to the same immobilized OSC<sup>pep</sup> if they are pre-incubated together (1 hr, room temperature) prior to binding in a solid-phase assay to the same immobilized OSC<sup>pep</sup>. These results show that OSCAR binding to its triple-helical collagen motif is dissociable.



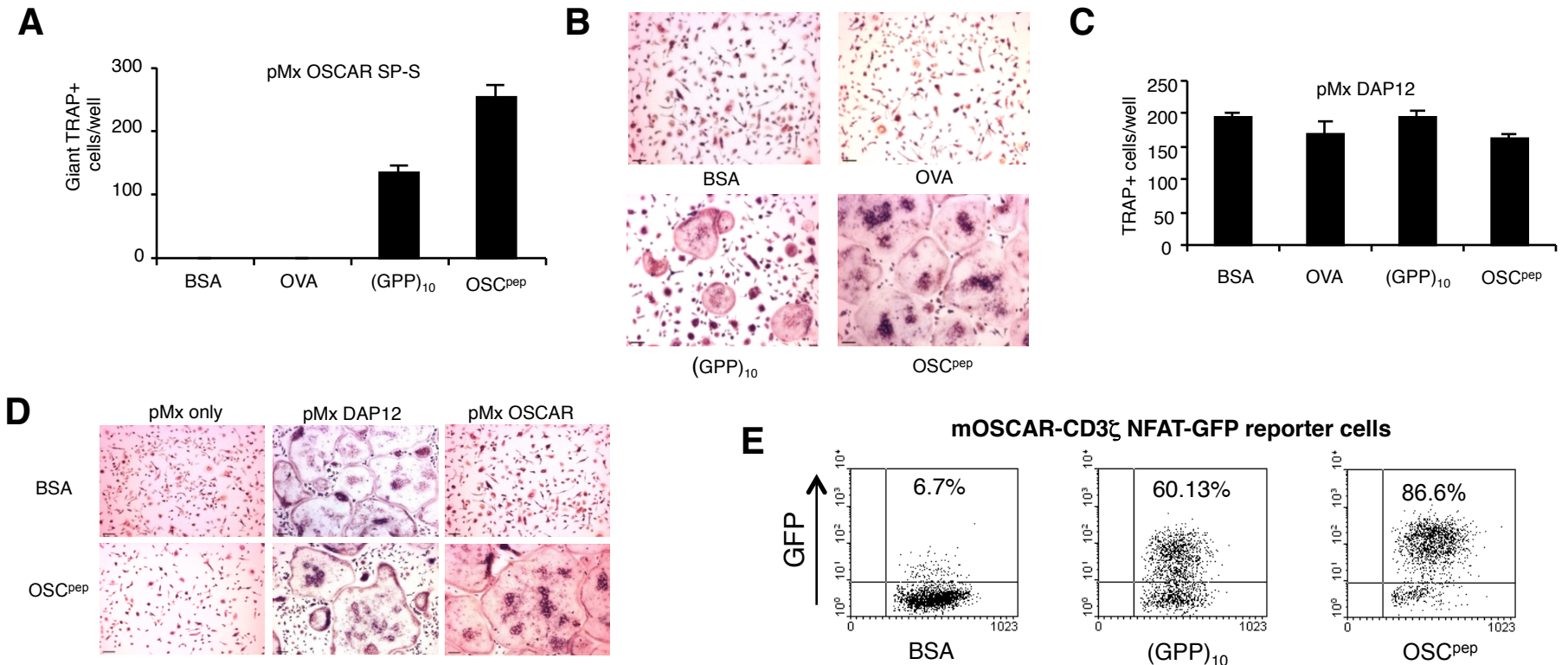
### Supplemental Figure 4

GFP expression of an OSCAR NFAT-GFP reporter cell-line cultured on immobilized collagen II and III toolkit peptides. Signaling, Mean Fluorescence Intensity (MFI) of GFP expression (y axis), induced by a hOSCAR-CD3 $\zeta$  NFAT-GFP reporter cell-line after overnight culture on tissue culture plates coated (x axis) with overlapping triple-helical peptides containing sequences from the collagen II and collagen III toolkits. Wells coated with either BSA or (GPP)<sub>10</sub>, were used as negative controls, and ProColl (a collagen I monomer – see methods), was used as positive control. The reasons for the imprecise fit between binding (Figure 3A) and activation signaling (GFP expression) between the two different techniques are not known. They may relate to threshold or sensitivity differences between the two assays e.g. addition of 0.05% Tween-20 in the solid-phase assay or the dimeric nature of hOSCAR-Fc compared to monomeric expression of hOSCAR-CD3 $\zeta$  protein. Although repeatable, the differences are not substantive.



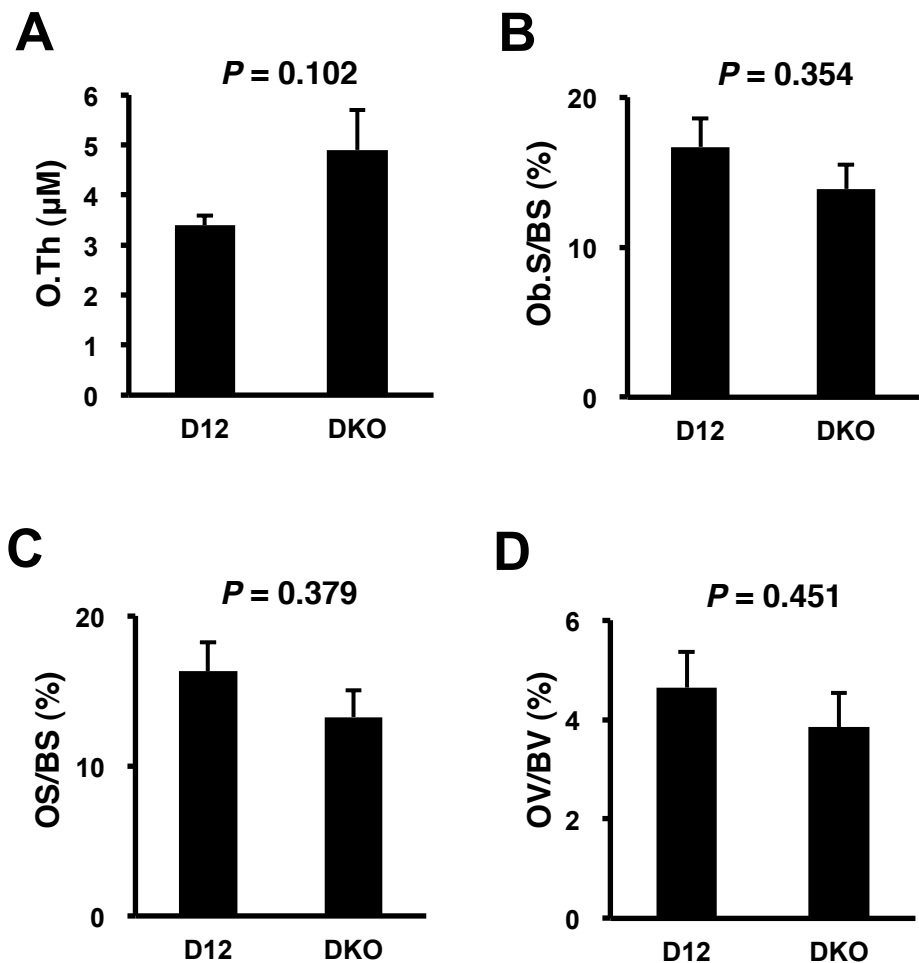
### Supplemental Figure 5

Immobilized OSC<sup>pep</sup> rescues the osteoclastogenesis defect of *DAP12<sup>-/-</sup>*, but not *DAP12<sup>-/-</sup>Oscar<sup>-/-</sup>*, BMMS. (A) Effect of immobilized proteins and peptides on RANKL differentiated *DAP12<sup>-/-</sup>* or *DAP12<sup>-/-</sup>Oscar<sup>-/-</sup>* BMM cultures. (B) Examples of giant TRAP+ multinucleated *DAP12<sup>-/-</sup>* cells formed on immobilized OSC<sup>pep</sup>, compared to mononuclear *DAP12<sup>-/-</sup>* cells in cultured on immobilized BSA, OVA or (GPP)<sub>10</sub> (Bar = 70 $\mu$ M). (C) TRAP staining of RANKL differentiated *DAP12<sup>-/-</sup>Oscar<sup>-/-</sup>* BMM cultured on immobilized proteins and peptides. Only mononuclear *DAP12<sup>-/-</sup>Oscar<sup>-/-</sup>* cells, like *DAP12<sup>-/-</sup>Fcer1g<sup>-/-</sup>* cells (data not shown and references 9 and 10) formed under the conditions tested, implying that the recognition of OSC<sup>pep</sup> is mediated by OSCAR (Bar = 70 $\mu$ M). Data are represented as mean (n=3)  $\pm$  SEM.



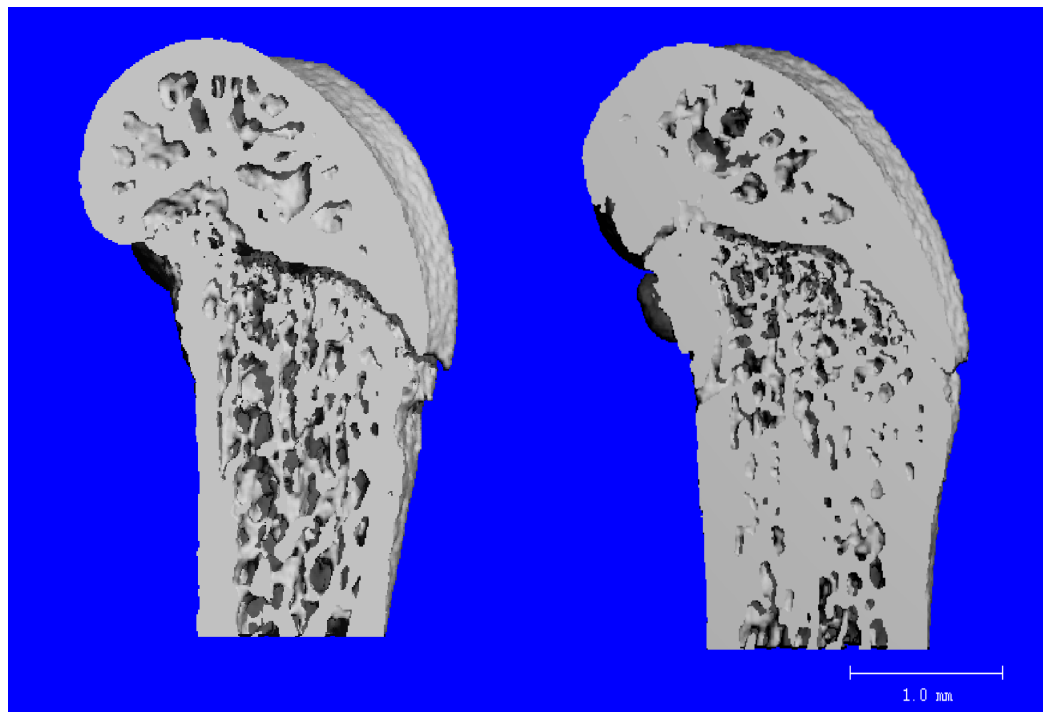
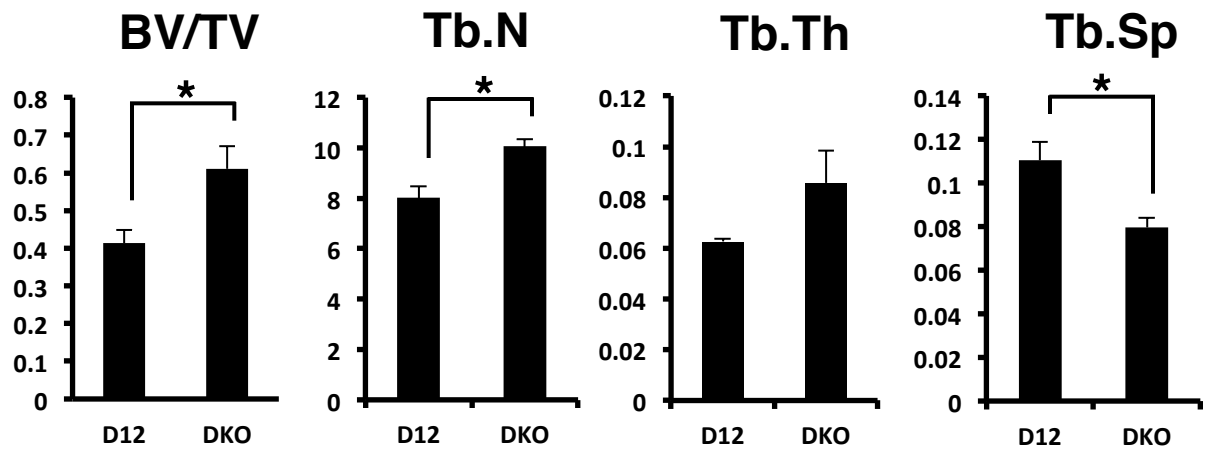
**Supplemental Figure 6**

Retroviral transduction of OSCAR rescues osteoclastogenesis of *DAP12*<sup>-/-</sup>*Oscar*<sup>-/-</sup> BMM cultured on immobilized OSC<sup>pep</sup>. (A) Effect of immobilized proteins and peptides on RANKL differentiated *DAP12*<sup>-/-</sup>*Oscar*<sup>-/-</sup> BMM retrovirally transduced with the short signal peptide isoform (SP-S) of murine OSCAR. Transduction of the long (SP-L, Figure 8D) or short signal peptide (SP-S) isoforms of murine OSCAR results in osteoclastogenesis on (GPP)<sub>10</sub> and OSC<sup>pep</sup>, respectively. It is notable that neither *DAP12*<sup>-/-</sup> BMM (Figure 8A; Supplemental Figure 5, A and B) nor *DAP12*<sup>-/-</sup>*Oscar*<sup>-/-</sup> BMM (Supplemental Figure 5, A and C), which express the endogenous murine OSCAR, formed giant TRAP<sup>+</sup> multinucleated cells on immobilized (GPP)<sub>10</sub>. (B) TRAP-stained *DAP12*<sup>-/-</sup>*Oscar*<sup>-/-</sup> BMM transduced with mouse OSCAR SP-S on either immobilized BSA, OVA, (GPP)<sub>10</sub> or OSC<sup>pep</sup>. (C) Quantification of rescued TRAP<sup>+</sup> giant multinucleated *DAP12*<sup>-/-</sup>*Oscar*<sup>-/-</sup> cells following retroviral transduction with pMx DAP12 and RANKL differentiation in wells coated with different immobilized peptides and proteins. (D) TRAP-staining of RANKL-differentiated *DAP12*<sup>-/-</sup>*Oscar*<sup>-/-</sup> BMM, after retroviral transduction with empty pMx vector (column 1), pMx DAP12 (column 2) or pMx vector encoding the long signal peptide isoform of OSCAR (column 3), cultured on plate-immobilized BSA (row 1) or OSC<sup>pep</sup> (row 2). (E) NFAT-GFP reporter cells retrovirally transduced with a murine (m)OSCAR-CD3 $\zeta$  construct were cultured overnight on immobilized BSA, (GPP)<sub>10</sub> or OSC<sup>pep</sup> and GFP expression was analysed by flow cytometry (y axis, GFP expression; x axis, forward scatter). Dotplots displaying 2000 events are shown. mOSCAR-CD3 $\zeta$  NFAT-GFP reporter cells expressed GFP after incubation on immobilized (GPP)<sub>10</sub> and OSC<sup>pep</sup>, but not BSA, showing retroviral over-expression of murine OSCAR results in signaling on immobilized (GPP)<sub>10</sub>. GFP expression detected in the upper quadrants are displayed as a percentage. Data are represented as mean (n=3)  $\pm$  SEM. Scale bars = 70 $\mu$ M.



**Supplemental Figure 7**

Histomorphometric osteoblast parameters. (A) Osteoid thickness (O.Th [ $\mu\text{M}$ ]). (B) Osteoblast surface/bone surface (Ob.S/BS [%]). (C) Osteoid surface/bone surface (OS/BS [%]) and (D) Osteoid volume/bone volume (OV/BV [%]) parameters for *DAP12*<sup>-/-</sup>, compared to *DAP12*<sup>-/-</sup>*Oscar*<sup>-/-</sup> (DKO), mice. Data are represented as mean ( $n=10$ )  $\pm$ SEM.  $P$ -values are indicated above each graph. No significant differences were observed in osteoblast parameters between *DAP12*<sup>-/-</sup> and *DAP12*<sup>-/-</sup>*Oscar*<sup>-/-</sup> mice.

**A***DAP12<sup>-/-</sup>**DKO***B****Supplemental Figure 8**

Increased bone mass of *DAP12<sup>-/-</sup>Oscar<sup>-/-</sup>* mice. (A) Representative 3-dimensional reconstruction of the femur (12 weeks old) by  $\mu$ CT from *DAP12<sup>-/-</sup>Oscar<sup>-/-</sup>* (DKO) and *DAP12<sup>-/-</sup>* mice. The marrow is filled with more unresorbed trabecular bone in DKO mice. (B) The percentage of trabecular bone volume/tissue volume (BV/TV), trabecular number (Tb.N), trabecular thickness (Tb.Th) and trabecular spacing (Tb.Sp), as determined by  $\mu$ CT. Data are represented as mean ( $n=5$ )  $\pm$ SEM; \* =  $P < 0.05$ .

Personal Reference	Amino-acid sequences of III-36 peptide derivatives, alanine scan and amino-acid substitutions.	Mass (Da)
NR315	GPC(GPP)5-GERGETGPOGPAGFOGAOGQN-(GPP)5GPC-NH2	5024
NR316	GPC(GPP)5-GPOGPAGFOGAOGQNGEoggk-(GPP)5GPC-NH2	4936
DB80	GPC(GPP)5-GPOGPAGFOGAO-(GPP)5GPC-NH2	4095
DB83	GPC(GPP)5-GAOGPAGFOGAO-(GPP)5GPC-NH2	4069
DB92	GPC(GPP)5-GPAGPAGFOGAO-(GPP)5GPC-NH2	4051
NR317	GPC(GPP)5-GPOGAAGFOGAO-(GPP)5GPC-NH2	4069
NR318	GPC(GPP)5-GPOGPAGAOGAO-(GPP)5GPC-NH2	4019
DB85	GPC(GPP)5-GPOGPAGFAGAO-(GPP)5GPC-NH2	4053
NR319	GPC(GPP)5-GPOGPAGFOGAA-(GPP)5GPC-NH2	4053
NR325	GPC(GPP)5-GAOGPAGFA-(GPP)5GPC-NH2	3786
NR328	GPC(GPP)5-GAOGPAGFA-(GPP)5GPC-NH2	3828
NR326	GPC(GPP)5-GAOGAAGFA-(GPP)5GPC-NH2	3760
NR327	GPC(GPP)5-GAOGPAGFA-(GPP)5GPC-NH2	3812
DB99	GPC(GPP)5-GAOGPAGSA-(GPP)5GPC-NH2	3726
NR330	GPC(GPP)5-GAOGPAGFD-(GPP)5GPC-NH2	3754
DB100	GPC(GPP)5-GAOGPAGEA-(GPP)5GPC-NH2	3768
DB101	GPC(GPP)5-GKOGPAGFA-(GPP)5GPC-NH2	3843
DB106	GPC(GPP)5-GAOGVMGFA-(GPP)5GPC-NH2	3848
DB107	GPC(GPP)5-GLOGPSGEO-(GPP)5GPC-NH2	3868
DB108	GPC(GPP)5-GFOGLOGPS-(GPP)5GPC-NH2	3886
DB109	GPC(GPP)5-GAOGPAGFAGEA-(GPP)5GPC-NH2	4043
DB110	GPC(GPP)5-GFOGPAGFA-(GPP)5GPC-NH2	3862
NR331	GPC(GPP)5-GQOOGPAGFA-(GPP)5GPC-NH2	3843
NR332	GPC(GPP)5-GEQGPAGFA-(GPP)5GPC-NH2	3844
NR334	GPC(GPP)5-GAOGPQQGFA-(GPP)5GPC-NH2	3843
NR335	GPC(GPP)5-GAOGPQQGPA-(GPP)5GPC-NH2	3793
NR338	GPC(GPP)5-GAOGASGDR-(GPP)5GPC-NH2	3829
NR340	GPC(GPP)5-GAOGPAGYA-(GPP)5GPC-NH2	3802
DB179	GPCGPOGPAGFOGPC-NH2	1341
DB187	GPC(GPP)5-GPOGPAGFO-(GPP)5GPC-NH2	3854
DB189	GPC(GPP)5-GAOGPAGFO-(GPP)5GPC-NH2	3828

**Supplemental Table 1**

List of the amino-acid sequences of the peptide III-36 derivatives, alanine scan and amino-acid substitutions. The laboratory reference number of each III-36 triple-helical peptide derivative series, corresponding amino-acid sequence and respective mass of the linear peptide in Daltons are indicated. X = substituted residue compare to parental OSCAR-binding sequence i.e. 'DB80' GPOGPAGFO(GAO). The collagen II and III toolkits have been described before (29, 30).